Acta Crystallographica Section A
Foundations of Crystallography
ISSN 0108-7673

Received 5 January 2010
Accepted 2 April 2010

© 2010 International Union of Crystallography
Printed in Singapore – all rights reserved

Three-beam X-ray rocking curves calculated from computer-simulated pinhole topographs

Gen Ishiwata,[a] Kouhei Okitsu[b]* and Makio Ishiguro[a]

[a]Department of Statistical Science, School of Multidisciplinary Science, The Graduate University for Advanced Studies (SOKENDAI), The Institute of Statistical Mathematics (ISM), 10-3 Midori-cho, Tachikawa, Tokyo 190-8562, Japan, and [b]Nano-Engineering Research Center, Institute of Engineering Innovation, Graduate School of Engineering, The University of Tokyo, 2-11-16 Yayoi, Bunkyo-ku, Tokyo 113-8656, Japan. Correspondence e-mail: okitsu@soyak.t.u-tokyo.ac.jp

X-ray rocking curves are reported which have been obtained by fast-Fourier-transforming X-ray amplitudes in three-beam pinhole topographs. The topographs were computer-simulated based on the Takagi–Taupin equation with the condition of spherical-wave X-ray incidence. This is another strategy for calculating three-beam rocking curves, which are usually calculated based on the Ewald–Laue dynamical theory.

1. Introduction

The *Pendellösung* fringes observed in X-ray section topographs have been explained by Kato's spherical-wave dynamical theory (Kato, 1961*a*,*b*, 1968*a*,*b*), which was derived based on the Ewald–Laue (E–L) dynamical theory (Ewald, 1917; von Laue, 1931). The E–L theory was extended to the three-beam case (Hildebrandt, 1967; Héno & Ewald, 1968; Ewald & Héno, 1968) in the late 1960s. X-ray intensities observed in experimentally obtained three-beam pinhole topographs were compared with computer-simulated topographs for the first time by Heyroth *et al.* (2001). Their simulated topographs were obtained by coherently superposing the plane-wave solutions of the three-beam E–L theory. Good agreements between experimentally obtained and computer-simulated images were reported. Studies of X-ray three-beam rocking curves are recognized to be very important, since phase information on crystal structure factors can be extracted from them (Colella, 1995*a*,*b*; Weckert & Hümmer, 1997, 1998; Shen & Wang, 2003; Chang, 2004).

On the other hand, X-ray amplitudes in section topographs calculated based on the Takagi–Taupin (T–T) equation (Takagi, 1962, 1969; Taupin, 1964) under the assumption of spherical-wave incidence are identical with those given by Kato's spherical-wave dynamical theory. Authier & Simon (1968) clarified the Fourier-transform relation between solutions of the T–T equation under the assumptions of plane- and spherical-wave incident X-rays. The T–T theory was extended to the three-beam case without taking into account the polarization effect by Thorkildsen (1987) and taking it into account by Larsen & Thorkildsen (1998). One of the present authors has extended the T–T theory into n-beam cases with n up to 12 (Okitsu, 2003). Okitsu and co-authors have given a numerical method for solving the equation and have reported good agreements between experimentally obtained and computer-simulated six-beam pinhole topographs (Okitsu *et al.*, 2003, 2006).

The E–L theory describes X-ray wavefields in a perfect crystal in reciprocal space. However, the behavior of X-rays in a perfect crystal can also be described by the T–T equation in real space. Because of this, the T–T equation has the significant capability of being able to deal with X-ray wavefields in a distorted crystal. Pioneering work to calculate two-beam rocking curves numerically based on the T–T equation for bent crystals (Taupin, 1964) was followed by work on silicon crystals with epilayers (Fukuhara & Takano, 1977*a*,*b*), ion-implanted garnet crystals (Takeuchi *et al.*, 1983) and crystals with surface acoustic waves (Gabrielyan & Aslanian, 1988).

In the present paper it is shown that the three-beam X-ray rocking curves for a perfect crystal can also be obtained from computer-simulated pinhole topographs based on the three-beam T–T equation.

2. A method for calculating X-ray rocking curves from computer-simulated three-beam pinhole topographs

In this section, a method for calculating rocking curves from X-ray amplitudes in computer-simulated three-beam pinhole topographs is described. For simplicity, the discussions are limited to a symmetrical transmission geometry for a parallel-sided crystal with a thickness of t. The amplitudes in real space of forward-diffracted ($p = o$) and reflected ($p = h, g$) X-rays on the exit surface of the crystal are represented as

$$D_p^{(l)}(\mathbf{r}_e)\exp(-i2\pi\mathbf{K}_p\cdot\mathbf{r}_e) = \int_{\Delta\mathbf{K}_p} \mathcal{D}_p^{(l)}(\Delta\mathbf{K}_p)\exp[-i2\pi(\mathbf{K}_p-\Delta\mathbf{K}_p)\cdot\mathbf{r}_e]\,\mathrm{d}\Delta\mathbf{K}_p, \quad (1)$$

where $p \in \{o, h, g\}$, $l \in \{\sigma, \pi\}$.

$D_p^{(l)}(\mathbf{r}_e)$ is the X-ray amplitude of the pth wave with polarization state of l at $\mathbf{r}_e$, where $\mathbf{r}_e$ is the location vector on the exit

surface of the crystal. $\mathbf{K}_p$ is $\overrightarrow{L_a H_p}$, where L_a is the Laue point and H_p is the reciprocal-lattice node. $\Delta\mathbf{K}_p$ is $\overrightarrow{L_a Q_p}$, where Q_p is a point on S_p. S_p is a plane normal to $\mathbf{K}_p$ whose distance from H_p is K, where K is the wavenumber of X-rays in vacuum. While Q_p is in fact on the surface of a sphere whose center is H_p and radius is K, the following discussions are described based on an approximation that Q_p is on S_p, since this situation is sufficiently satisfied in the vicinity of the exact three-beam condition. $\mathcal{D}_p^{(l)}(\Delta\mathbf{K}_p)$ is the amplitude of X-rays whose wavevector is $\mathbf{K}_p - \Delta\mathbf{K}_p$. $\int_{\Delta\mathbf{K}_p} \mathrm{d}\mathbf{K}_\mathrm{p}$ means integration over S_p. Now let us define unit vectors $\mathbf{s}_p$, $\mathbf{e}_p^{(\sigma)}$ and $\mathbf{e}_p^{(\pi)}$ as

$$\begin{aligned}\mathbf{s}_p &= \mathbf{K}_p/K,\\ \mathbf{e}_p^{(\sigma)} &= \frac{\mathbf{s}_p \times [\mathbf{s}_{(p+1)'} - \mathbf{s}_p]}{|\mathbf{s}_p \times [\mathbf{s}_{(p+1)'} - \mathbf{s}_p]|},\\ \mathbf{e}_p^{(\pi)} &= \mathbf{s}_p \times \mathbf{e}_p^{(\sigma)}.\end{aligned}$$

Here, $(p+1)'$ is h, g and o when p is o, h and g, respectively. Substituting $\mathbf{r}_\mathrm{e} = s_p\mathbf{s}_p + e_p^{(\sigma)}\mathbf{e}_p^{(\sigma)} + e_p^{(\pi)}\mathbf{e}_p^{(\pi)}$ and $\Delta\mathbf{K}_p = \eta_p^{(\sigma)}\mathbf{e}_p^{(\sigma)} + \eta_p^{(\pi)}\mathbf{e}_p^{(\pi)}$ into equation (1), the following equation can be obtained:

$$D_p^{(l)}(\mathbf{r}_\mathrm{e}) = \int_{-\infty}^{\infty}\int_{-\infty}^{\infty} \mathcal{D}_p^{(l)}(\Delta\mathbf{K}_p) \times \exp\left[i2\pi(\eta_p^{(\sigma)}e_p^{(\sigma)} + \eta_p^{(\pi)}e_p^{(\pi)})\right] \mathrm{d}\eta_p^{(\sigma)}\,\mathrm{d}\eta_p^{(\pi)}. \quad (2)$$

Therefore, the X-ray amplitude $\mathcal{D}_p^{(l)}(\Delta\mathbf{K}_p)$ in reciprocal space is represented by Fourier-transforming $D_p^{(l)}(\mathbf{r}_\mathrm{e})$ as

$$\mathcal{D}_p^{(l)}(\Delta\mathbf{K}_p) = (1/2\pi) \int_{\mathrm{Min}(e_p^{(\pi)})}^{\mathrm{Max}(e_p^{(\pi)})}\int_{\mathrm{Min}(e_p^{(\sigma)})}^{\mathrm{Max}(e_p^{(\sigma)})} D_p^{(l)}(\mathbf{r}_\mathrm{e}) \times \exp\left[-i2\pi(\eta_p^{(\sigma)}e_p^{(\sigma)} + \eta_p^{(\pi)}e_p^{(\pi)})\right] \mathrm{d}e_p^{(\sigma)}\,\mathrm{d}e_p^{(\pi)}. \quad (3)$$

Whereas the integration range of a Fourier transform is infinite in general, integration over a finite range is sufficient because $D_p^{(l)}(\mathbf{r}_\mathrm{e})$ has a nonzero value only inside the bottom of the Borrmann pyramid in the present case.

Incidentally, X-ray amplitudes in three-beam pinhole topographs computer-simulated with the same procedure as described in Okitsu *et al.* (2006) are obtained for a location on the exit surface of the crystal: $\mathbf{r}_\mathrm{e} = i\mathbf{a} + j\mathbf{b}$, where i and j are integers. Here, $\mathbf{a}$ and $\mathbf{b}$ are defined by

$$\mathbf{a} = (\mathbf{s}_g - \mathbf{s}_o)\frac{t}{n\cos\theta_\mathrm{B}}, \quad (4)$$

$$\mathbf{b} = (\mathbf{s}_h - \mathbf{s}_o)\frac{t}{n\cos\theta_\mathrm{B}}, \quad (5)$$

where n is the number of layers, each of which has thickness t/n. The three-beam T–T equation has been solved layer by layer, with layer thickness t/n, to obtain X-ray amplitudes on the exit surface. θ_B is the angle spanned by vectors $\mathbf{n}$ and $\mathbf{s}_p$, where $\mathbf{n}$ is the downward surface normal vector of the crystal defined by $\mathbf{n} = \mathbf{a}\times\mathbf{b}/|\mathbf{a}\times\mathbf{b}|$. For practical computer simulation of a pinhole topograph, $D_p'^{(l)}(i,j)$ is defined such that $D_p'^{(l)}(i,j) = D_p^{(l)}(i\mathbf{a} + j\mathbf{b})\left[= D_p^{(l)}(\mathbf{r}_\mathrm{e})\right]$. Further, $D_p'^{(l)}(i,j)$ should be projected onto S_p. Let us define $\mathbf{a}_p$ and $\mathbf{b}_p$ by projecting $\mathbf{a}$ and $\mathbf{b}$ onto S_p as follows:

$$\begin{aligned}\mathbf{a}_p &= \mathbf{a} + A_p\mathbf{s}_p\\ &= A_p^{(\sigma)}\mathbf{e}_p^{(\sigma)} + A_p^{(\pi)}\mathbf{e}_p^{(\pi)}, \quad (6)\end{aligned}$$

$$\begin{aligned}\mathbf{b}_p &= \mathbf{b} + B_p\mathbf{s}_p\\ &= B_p^{(\sigma)}\mathbf{e}_p^{(\sigma)} + B_p^{(\pi)}\mathbf{e}_p^{(\pi)}. \quad (7)\end{aligned}$$

Here $A_p, B_p, A_p^{(l)}$ and $B_p^{(l)}$ ($l \in \{\sigma,\pi\}$) are coefficients with dimension m and can be obtained by solving equations (6) and (7). Then $D_p'^{(l)}(i,j)$ is projected to position $\mathbf{r}_p = i\mathbf{a}_p + j\mathbf{b}_p$ on S_p. Next, reciprocal vectors $\mathbf{a}_p^*$ and $\mathbf{b}_p^*$ on S_p are defined as

$$\begin{aligned}\mathbf{a}_p^* &= -\frac{\mathbf{s}_p\times\mathbf{b}_p}{\mathbf{s}_p\cdot(\mathbf{a}_p\times\mathbf{b}_p)M}\\ &= A_p^{*(\sigma)}\mathbf{e}_p^{(\sigma)} + A_p^{*(\pi)}\mathbf{e}_p^{(\pi)}, \quad (8)\end{aligned}$$

$$\begin{aligned}\mathbf{b}_p^* &= \frac{\mathbf{s}_p\times\mathbf{a}_p}{\mathbf{s}_p\cdot(\mathbf{a}_p\times\mathbf{b}_p)N}\\ &= B_p^{*(\sigma)}\mathbf{e}_p^{(\sigma)} + B_p^{*(\pi)}\mathbf{e}_p^{(\pi)}, \quad (9)\end{aligned}$$

such that $\mathbf{a}_p\cdot\mathbf{a}_p^* = 1/M$, $\mathbf{b}_p\cdot\mathbf{b}_p^* = 1/N$ and $\mathbf{a}_p\cdot\mathbf{b}_p^* = \mathbf{b}_p\cdot\mathbf{a}_p^* = 0$, where M and N are numbers in summations that will appear in (10). Here, $A_p^{*(l)}$ and $B_p^{*(l)}$ are coefficients with dimension of m^{-1} which can be obtained by solving equations (8) and (9). Because equation (3) is satisfied even if $\mathbf{r}_\mathrm{e}$ is replaced by $\mathbf{r}_p$, $\mathcal{D}_p'^{(l)}(k_i,k_j)$ at position $k_i\mathbf{a}_p^* + k_j\mathbf{b}_p^*$ in the two-dimensional reciprocal space on S_p can be obtained by

$$\mathcal{D}_p'^{(l)}(k_i,k_j) = \frac{\mathbf{s}_p\cdot(\mathbf{a}_p\times\mathbf{b}_p)}{2\pi}\sum_{i=\mathrm{Min}(i)}^{\mathrm{Max}(i)}\sum_{j=\mathrm{Min}(j)}^{\mathrm{Max}(j)} D_p'^{(l)}(i,j) \times \exp\left[-i2\pi(ik_i/M + jk_j/N)\right], \quad (10)$$

where $M = \mathrm{Max}(i) - \mathrm{Min}(i) + 1$, $N = \mathrm{Max}(j) - \mathrm{Min}(j) + 1$.

To obtain the rocking curves as a function of $\Delta\omega$ and $\Delta\psi$, which are rotation angles of the crystal around the $\mathbf{e}_o^{(\sigma)}$ and $\mathbf{e}_o^{(\pi)}$ axes, projections of $\omega_\mathrm{step}K\mathbf{e}_o^{(\pi)}$ and $\psi_\mathrm{step}K\mathbf{e}_o^{(\sigma)}$ on S_p should be considered. Here ω_step and ψ_step are angular steps when rotating the crystal around the $\mathbf{e}_o^{(\sigma)}$ and $\mathbf{e}_o^{(\pi)}$ axes, respectively. These vectors $\mathbf{a}_p^{*\prime}$ and $\mathbf{b}_p^{*\prime}$ projected on S_p can be calculated by

$$\begin{aligned}\mathbf{a}_p^{*\prime} &= \omega_\mathrm{step}K\mathbf{e}_o^{(\sigma)} + A_p^{*\prime}\mathbf{n}\\ &= A_p^{*\prime(\sigma)}\mathbf{e}_p^{(\sigma)} + A_p^{*\prime(\pi)}\mathbf{e}_p^{(\pi)}, \quad (11)\end{aligned}$$

$$\begin{aligned}\mathbf{b}_p^{*\prime} &= \psi_\mathrm{step}K\mathbf{e}_o^{(\pi)} + B_p^{*\prime}\mathbf{n}\\ &= B_p^{*\prime(\sigma)}\mathbf{e}_p^{(\sigma)} + B_p^{*\prime(\pi)}\mathbf{e}_p^{(\pi)}. \quad (12)\end{aligned}$$

Here $A_p^{*\prime}$, $B_p^{*\prime}$, $A_p^{*\prime(l)}$ and $B_p^{*\prime(l)}$ are coefficients with dimension m^{-1} which can be obtained by solving equations (11) and (12). $\mathcal{D}_p'^{(l)}(k_i,k_j)$ can be transformed to $\mathcal{D}_p''^{(l)}(\Delta\omega,\Delta\psi)$ as a function of $\Delta\omega$ ($= k_i'\omega_\mathrm{step}$) and $\Delta\psi$ ($= k_j'\psi_\mathrm{step}$), where k_i' and k_j' are no longer integers. Because $k_i\mathbf{a}_p^* + k_j\mathbf{b}_p^* = k_i'\mathbf{a}_p^{*\prime} + k_j'\mathbf{b}_p^{*\prime}$, the relation between k_i, k_j and k_i', k_j' is represented as

$$\mathbf{M}\mathbf{X} = \mathbf{M}'\mathbf{X}',$$

where

$$\mathbf{M} = \begin{pmatrix} A_p^{*(\sigma)} & B_p^{*(\sigma)} \\ A_p^{*(\pi)} & B_p^{*(\pi)} \end{pmatrix}, \quad \mathbf{X} = \begin{pmatrix} k_i \\ k_j \end{pmatrix},$$

Table 1
Parameters of X-ray reflection indices of a silicon crystal.

The parameters were calculated for a photon energy of 12.0 keV using *XINPRO* of *XOP 2.11*; θ_B is the Bragg reflection angle and $|\chi_{hr}|$ and $|\chi_{hi}|$ are the absolute values of the real and imaginary parts of χ_h. Here χ_h is the hth-order Fourier coefficient of electric susceptibility. $\Lambda_L^{(\sigma)}$ and $\Lambda_L^{(\pi)}$ are the *Pendellösung* distances for transmission geometry defined in Authier (2004) for σ- and π-polarized X-rays in the two-beam case.

h	θ_B (°)	$\lvert\chi_{hr}\rvert \times 10^6$	$\lvert\chi_{hi}\rvert \times 10^8$	$\Lambda_L^{(\sigma)}$ (μm)	$\Lambda_L^{(\pi)}$ (μm)
000	0	6.77391	7.19974	15.25	15.25
044	32.5539	2.63570	6.33738	33.03	78.48
440	32.5539	2.63570	6.33738	33.03	78.48

$$\mathbf{M}' = \begin{pmatrix} A_p^{*\prime(\sigma)} & B_p^{*\prime(\sigma)} \\ A_p^{*\prime(\pi)} & B_p^{*\prime(\pi)} \end{pmatrix}, \quad \mathbf{X}' = \begin{pmatrix} k_i' \\ k_j' \end{pmatrix}.$$

Therefore, k_i' and k_j' can be obtained by $\mathbf{X}' = \mathbf{M}'^{-1}\mathbf{M}\mathbf{X}$.

Three-beam rocking curves can also be calculated by solving the eigenvalue/eigenvector problem of the three-beam E–L theory as described in Colella (1974). Values of ω_{step} and ψ_{step} in equations (11) and (12) should be sufficiently small to obtain two-dimensional rocking curves that are precise enough. Simultaneously, the value of t/n should be sufficiently small compared with the *Pendellösung* distance $\Lambda_L^{(l)}$ (see Table 1) to calculate the X-ray amplitudes in the pinhole topographs. In the cases of both Figs. 1 and 2, M and N in equations (8) and (9) were set to be $M = N = 8192$ ($= 2^{13}$) to satisfy the above two requirements simultaneously and to use the fast-Fourier-transform algorithm (Cooley & Tukey, 1965). Min(k) and Max(k) ($k \in \{i, j\}$) were adjusted such that the triangular region corresponding to the bottom of the Borrmann pyramid was placed in the central part of the summation range in equation (10).

3. Results and discussion

Figs. 1 and 2 show X-ray rocking curves of the h wave that were calculated based on the E–L theory, $[X(a)]$ ($X \in \{P, S\}$), and by fast-Fourier-transforming the X-ray amplitudes in computer-simulated pinhole topographs, $[X(b)]$. A symmetrical transmission geometry of the three-beam case with h = 044, g = 440 and incident X-rays π-polarized for $[P(x)]$ ($x \in \{a, b\}$) and σ-polarized for $[S(x)]$ were assumed for both Figs. 1 and 2. The three-beam T–T equation was solved in the same way as described in Okitsu *et al.* (2006) to obtain the X-ray amplitudes in pinhole topographs. The values of t and n in equations (4) and (5) were t = 75 μm and n = 1023 for Fig. 1, and t = 7.5 μm and n = 1023 for Fig. 2. The reflection parameters calculated by using *XINPRO* of *XOP 2.11* (Sanchez del Rio & Dejus, 1998) are summarized in Table 1 and were

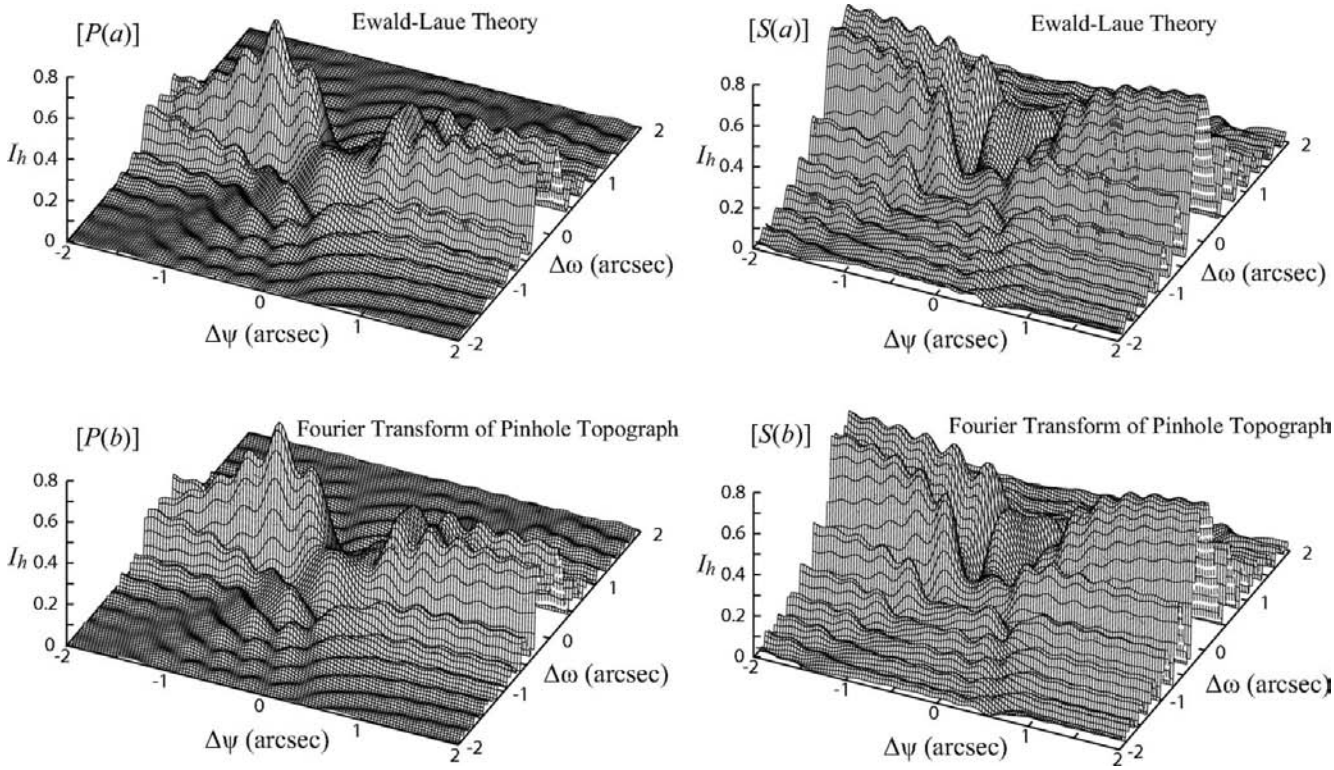

Figure 1
X-ray three-beam rocking curves of the h wave at a photon energy of 12 keV (wavelength 1.033 Å) for a symmetrical transmission geometry obtained by $[X(a)]$ ($X \in \{P, S\}$) solving the eigenvalue/eigenvector problem of the three-beam Ewald–Laue dynamical theory and $[X(b)]$ fast-Fourier-transforming X-ray amplitudes on the exit surface of the crystal of three-beam pinhole topographs which have been computer-simulated based on the Takagi–Taupin equation. X-rays π-polarized for $P(x)$ ($x \in \{a, b\}$) and σ-polarized for $S(x)$ incident on a silicon crystal with a thickness t = 75 μm were assumed. Angular variables $\Delta\omega$ and $\Delta\psi$ are presented in arcsec. I_h is the reflectivity defined by $I_h = |\mathcal{D}_h''^{(\sigma)}(\Delta\omega, \Delta\psi)|^2 + |\mathcal{D}_h''^{(\pi)}(\Delta\omega, \Delta\psi)|^2$, where $\Delta\omega = k_i'\omega_{step}$ and $\Delta\psi = k_j'\psi_{step}$.

used for the calculations. Signs of the angular deviations $\Delta\omega$ and $\Delta\psi$ were taken to be positive when the reflection angles of the h or g reflections were higher than the exact three-beam condition. In both Figs. 1 and 2, the reflectivity I_h was defined by $I_h = |\mathcal{D}_h^{\prime\prime(\sigma)}(\Delta\omega, \Delta\psi)|^2 + |\mathcal{D}_h^{\prime\prime(\pi)}(\Delta\omega, \Delta\psi)|^2$, where $\Delta\omega = k_i'\omega_{\rm step}$ and $\Delta\psi = k_j'\psi_{\rm step}$. Good agreements were found between $[X(a)]$ and $[X(b)]$ ($X \in \{P, S\}$) in both Figs. 1 and 2.

It has been pointed out by Weckert & Hümmer (1998) that t should be sufficiently small compared with the *Pendellösung* distance $\Lambda_L^{(l)}$ ($l \in \{\sigma, \pi\}$) if phase information is to be extracted from the three-beam rocking curves. While the case of Fig. 1 does not satisfy this requirement, the case of Fig. 2 does.

It has been shown that three-beam rocking curves for a perfect crystal, which are usually calculated based on the E–L theory, can also be computed by Fourier-transforming the amplitudes in computer-simulated pinhole topographs based on the T–T equation, at least for a symmetrical transmission geometry. The method using the T–T equation is able to deal with an arbitrary-shaped crystal, whereas the E–L theory can only deal with a semi-infinite perfect crystal with planar surfaces. The three-beam T–T equation can deal with cases in which transmission and reflection geometries coexist. Furthermore, this method for obtaining X-ray rocking curves is expected to be applicable to any n-beam ($n \in \{3, 4, 5, 6, 8, 12\}$) cases.

4. Conclusion

It has been shown that three-beam X-ray rocking curves can also be calculated by fast-Fourier-transforming X-ray amplitudes in computer-simulated pinhole topographs based on the three-beam T–T equation. With this method it is possible to deal with an arbitrary-shaped crystal when phase information on crystal structure factors is to be extracted by using the three-beam method.

The super computers HP-XC4000 (ismxc), HITACHI-SR11000 (ismsr), NEC-SX6 (ismsx), SGI-ALTIX3700 (ismaltix), SGI-PRISM (ismprsm), Fujitsu-PRIMERGY (ismrx) and Fujitsu-SPARC-Enterprise (isment) of the Institute of Statistical Mathematics and HITACHI-SR11000 (sumire) of the Institute for Solid State Physics of the University of Tokyo were used in the present work.

References

Authier, A. (2004). *Dynamical Theory of X-ray Diffraction*, revised ed. Oxford University Press.
Authier, A. & Simon, D. (1968). *Acta Cryst.* A**24**, 517–526.
Chang, S.-L. (2004). *X-ray Multiple-Wave Diffraction, Theory and Application.* New York: Springer.
Colella, R. (1974). *Acta Cryst.* A**30**, 413–423.
Colella, R. (1995*a*). *Comments Condens. Matter Phys.* **17**, 175–198.
Colella, R. (1995*b*). *Comments Condens. Matter Phys.* **17**, 199–215.
Cooley, J. W. & Tukey, J. W. (1965). *Math. Comput.* **19**, 297–301.

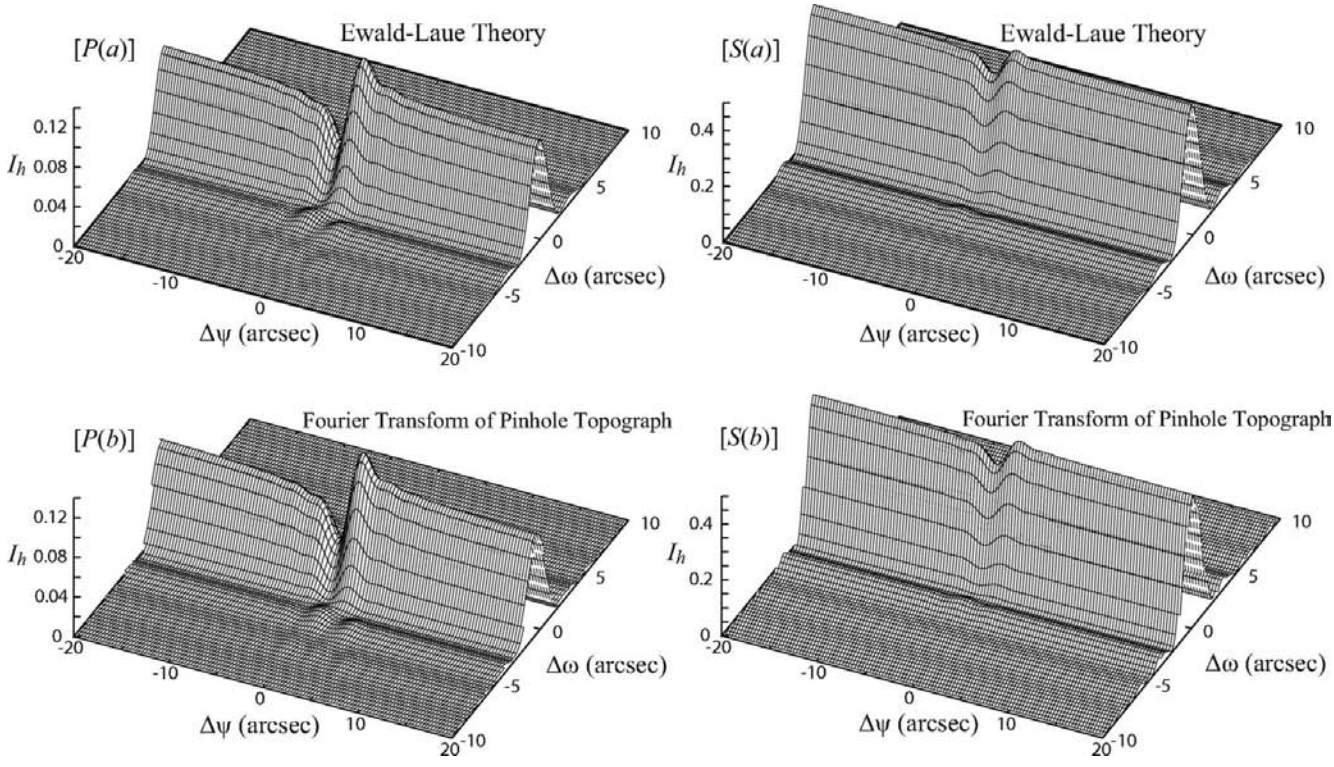

Figure 2
Three-beam rocking curves of the h beam. The crystal thickness t = 7.5 µm, in which the condition that t is sufficiently smaller than the *Pendellösung* distance $\Lambda_L^{(l)}$ ($l \in \{\sigma, \pi\}$, see Table 1) is satisfied (Weckert & Hümmer, 1998). The other assumed conditions are identical with those for Fig. 1. $[P(x)]$ and $[S(x)]$ ($x \in \{a, b\}$) correspond to $[P(x)]$ and $[S(x)]$ of Fig. 1.

Ewald, P. P. (1917). *Ann. Phys. 4. Folge*, **54**, 519–597.
Ewald, P. P. & Héno, Y. (1968). *Acta Cryst.* A**24**, 5–15.
Fukuhara, A. & Takano, Y. (1977*a*). *Acta Cryst.* A**33**, 137–142.
Fukuhara, A. & Takano, Y. (1977*b*). *J. Appl. Cryst.* **10**, 287–290.
Gabrielyan, K. T. & Aslanian, H. A. (1988). *Phys. Status Solidi A*, **108**, K85–K88.
Héno, Y. & Ewald, P. P. (1968). *Acta Cryst.* A**24**, 16–42.
Heyroth, F., Zellner, J., Höche, H.-R., Eisenschmidt, C., Weckert, E. & Drakopoulous, M. (2001). *J. Phys. D Appl. Phys.* **34**, A151–A157.
Hildebrandt, G. (1967). *Phys. Status Solidi*, **24**, 245–261.
Kato, N. (1961*a*). *Acta Cryst.* **14**, 526–532.
Kato, N. (1961*b*). *Acta Cryst.* **14**, 627–636.
Kato, N. (1968*a*). *J. Appl. Phys.* **39**, 2225–2230.
Kato, N. (1968*b*). *J. Appl. Phys.* **39**, 2231–2237.
Larsen, H. B. & Thorkildsen, G. (1998). *Acta Cryst.* A**54**, 129–136.
Laue, M. von (1931). *Ergeb. Exakten Naturwiss.* **10**, 133–158.
Okitsu, K. (2003). *Acta Cryst.* A**59**, 235–244.
Okitsu, K., Imai, Y., Ueji, Y. & Yoda, Y. (2003). *Acta Cryst.* A**59**, 311–316.
Okitsu, K., Yoda, Y., Imai, Y., Ueji, Y., Urano, Y. & Zhang, X. (2006). *Acta Cryst.* A**62**, 237–247.
Sanchez del Rio, M. & Dejus, R. J. (1998). *Proc. SPIE*, **3448**, 340–345.
Shen, Q. & Wang, J. (2003). *Acta Cryst.* D**59**, 809–814.
Takagi, S. (1962). *Acta Cryst.* **15**, 1311–1312.
Takagi, S. (1969). *J. Phys. Soc. Jpn*, **26**, 1239–1253.
Takeuchi, T., Ohta, N., Sugita, Y. & Fukuhara, A. (1983). *J. Appl. Phys.* **54**, 715–721.
Taupin, D. (1964). *Bull. Soc. Fr. Minéral. Cristallogr.* **87**, 469–511.
Thorkildsen, G. (1987). *Acta Cryst.* A**43**, 361–369.
Weckert, E. & Hümmer, K. (1997). *Acta Cryst.* A**53**, 108–143.
Weckert, E. & Hümmer, K. (1998). *Cryst. Res. Technol.* **33**, 653–678.